Supplementary for

Estimation of future changes in photovoltaic potential in Australia due to climate change

Shukla Poddar[1,2], Jason P Evans[2,3], Merlinde Kay[1], Abhnil Prasad[1,2,3], Stephen Bremner[1]

[1]School of Photovoltaic and Renewable Energy Engineering, University of New South Wales, Sydney, Australia

[2]ARC Centre of Excellence for Climate Extremes

[3]Climate Change Research Centre, Biological, Earth and Environmental Sciences, University of New South Wales, Sydney, Australia

Corresponding author: Shukla Poddar (s.poddar@unsw.edu.au)

Contents of this file

Table s1

Figures s1 to s5

Introduction

This supporting information includes:

- A table containing the details of the parameterization schemes used for creating different NARCliM ensemble members.
- Derivation of net change in PV potential due to contribution of radiation, temperature and wind speed.
- Cell efficiency loss threshold temperature.
- A figure representing the relationship of PV cell relative efficiency with irradiance, temperature and cell temperature (Figure s1).
- A figure representing the changes in the PV potential due to radiation, temperature and wind speed (Figure s2).
- A figure similar to figure 4(a-c) from the article demonstrating the mean cell temperature over Australia for the historical period and its changes for the near future and far future periods (Figure s3).
- A figure representing the cell efficiency losses for historical period and changes in the cell efficiency loss in the future periods (Figure s4).
- A figure similar to figure 4(g-i) from the article demonstrating the number of days/year there shall be a 16-19% efficiency loss during the historical period and the expected changes for the near and far future periods (Figure s5).

1. Parameterization schemes used for different ensemble members

***Table s1**: WRF schemes selected to generate the RCMs*

Ensemble Member	Planetary boundary layer physics/ surface layer physics	Cumulus physics	Microphysics	Shortwave/long-wave radiation physics	Land Surface
R1	MYJ /Eta similarity	Kain–Fritsch	WDM5	Dudhia/RRTM	Noah LSM
R2	MYJ /Eta similarity	Betts–Miller–Janjic	WDM5	Dudhia/RRTM	Noah LSM
R3	YSU/MM5 similarity	Kain–Fritsch	WDM5	CAM/CAM	Noah LSM

Table s1 describes the different parameterization schemes chosen to downscale four global climate models (GCMs) using three Weather Research Forecasting v3.3 (WRF) model configurations (Evans et al., 2014). The GCMs are chosen from the Coupled Model Intercomparison Project phase 3 (CMIP3) archive (MIROC3.2, ECHAM5, CCCMA3.1 and CSIRO-MK3.0). Thus the final ensemble contains 12 members (4 GCMs x 3 RCMs).

2. Contribution of climate variables in PV potential change

$$PV\ Potential\ (P) = \mathrm{P_R} \times {}^{\mathrm{G}}/_{\mathrm{G_{STC}}} \ldots\ldots\ldots\ldots\ldots\ldots eq\ 1$$

where G_{STC}=1000 W/m^2

$$P_R = 1 + \gamma\left(T_{cell} - T_{ref}\right) \ldots\ldots\ldots\ldots\ldots\ldots.eq\ 2$$

where T_{ref}= 25 °C

$$T_{cell} = C_1 + C_2T + C_3G + C_4V \ldots\ldots\ldots\ldots\ldots\ldots eq\ 3$$

where C_1, C_2, C_3 and C_4 are taken as 4.3 ºC, 0.943, 0.028 ºC m^2 W^{-1} and -1.528 ºCs m^{-1} respectively.

Combining equation 2 and 3 in 1,

$$P = 1 + \gamma\left((C_1 + C_2T + C_3G + C_4V) - T_{ref}\right) x\ {}^{\mathrm{G}}/_{\mathrm{G_{STC}}} \ldots\ldots\ldots\ldots\ldots\ldots eq\ 4$$

Adding values of G_{STC}, T_{ref}, γ, C_1, C_2, C_3 and C_4 to equation 4 we get,

$$PV_{pot} = \alpha_1 + \alpha_2G^2 + \alpha_3GT + \alpha_4GV \ldots\ldots\ldots\ldots\ldots\ldots eq\ 5$$

where $\alpha_1 = 1.1035 \times 10^{-3}(W/m^2)^{-1}$, $\alpha_2 = -1.4 \times 10^{-7}(W/m^2)^{-2}$, $\alpha_3 = -4.715 \times 10^{-6}$(W°C /m^2)$^{-1}$ and $\alpha_4 = 7.64 \times 10^{-6}(W/ms)^{-1}$

Using Taylor expansion in equation 5 we obtain the net change in PV potential due to radiation, temperature and wind speed,

$$\Delta PV_{pot} = \Delta G(\alpha_1 + \alpha_2\Delta G + 2\alpha_2G + \alpha_3T + \alpha_4V) + \alpha_3G\Delta T + \alpha_4G\Delta V + \alpha_3\Delta G\Delta T + \alpha_4\Delta G\Delta V \ldots\ldots\ldots\ldots\ldots\ldots eq\ 6$$

where ΔT, ΔG and ΔV are the changes in temperature, radiation and wind between the historical and the future period

The change in PV potential due to the change in radiation only is obtained from equation 6 (considering ΔT=ΔV=0):

$$\Delta PV_{pot_R} = \Delta G(\boldsymbol{\alpha}_1 + \alpha_2\Delta G + 2\alpha_2 G + \alpha_3 T + \alpha_4 V) \ldots\ldots\ldots\ldots\ldots\ldots eq\ 7$$

The change in PV potential due to the change in temperature only is obtained from equation 6 (considering ΔG=ΔV=0):

$$\Delta PV_{pot_T} = \alpha_3 G \Delta \mathrm{T} \ldots\ldots\ldots\ldots\ldots\ldots eq\ 8$$

The change in PV potential due to the change in wind only is obtained from equation 6 (ΔT=ΔG =0):

$$\Delta PV_{pot_V} = \alpha_4 G \Delta \mathrm{V} \ldots\ldots\ldots\ldots\ldots\ldots eq\ 9$$

3. Cell efficiency loss threshold temperature

Cell efficiency is calculated using: $\eta c \; = \eta t \; [1 - \beta(T\_cell - T\_ref\;)] \ldots \ldots \ldots \ldots \ldots \ldots eq\; 10$

where T_{cell} and T_{ref} are the cell temperature and reference temperature respectively. ηt is the rated power conversion efficiency of the solar cell at reference temperature. β is efficiency temperature coefficient (0.45%/℃) (Kaldellis et al., 2014; Makrides et al., 2012).

To estimate the cell efficiency loss of 15%, we find consider: $\frac{\eta t - \eta c}{\eta t} \times 100 = 15\%$.

On re-arranging the equation 10,

$$1 - \frac{\eta c}{\eta t} = 1 - [1 - \beta\left(T_{cell} - T_{ref}\right)] \ldots\ldots\ldots\ldots\; eq\; 11$$

On adding all the values of the constants to equation 11, we can solve for T_{cell} = 58.33 ℃ for 15% loss. Similarly, threshold temperature is found to be 60.55 ℃, 62.77 ℃, 65 ℃ and 67.22 ℃ for 16%, 17% 18% and 19% loss respectively.

4. Relationship of PV cell relative efficiency with irradiance, temperature and cell temperature

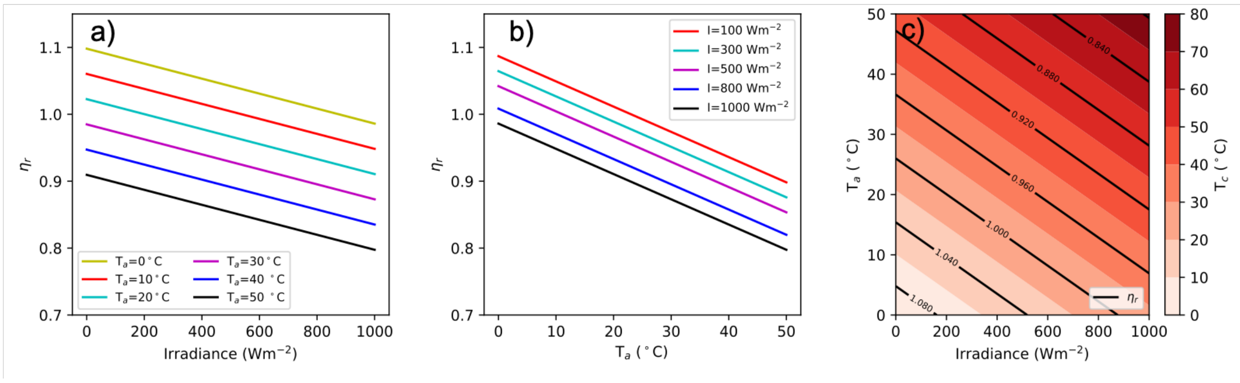

Figure s1. *Relationship of relative efficiency with a) irradiance b) ambient temperature c) variation of cell temperature with irradiance and ambient air temperature.*

It can be noted that relative cell efficiency (η_r) decreases with an increase in ambient temperature at constant irradiance level. Cell temperature increases with an increase in the ambient temperature and irradiance. η_r also decreases with an increase in the cell temperature. There is an agreement with the previous literature (Chander et al., 2015; Notton et al., 2005) where they have reported similar relationship of relative cell efficiency with ambient temperature and irradiance.

5. Change in the net PV potential over Australia for the near future and far future periods due to radiation, temperature and wind speed

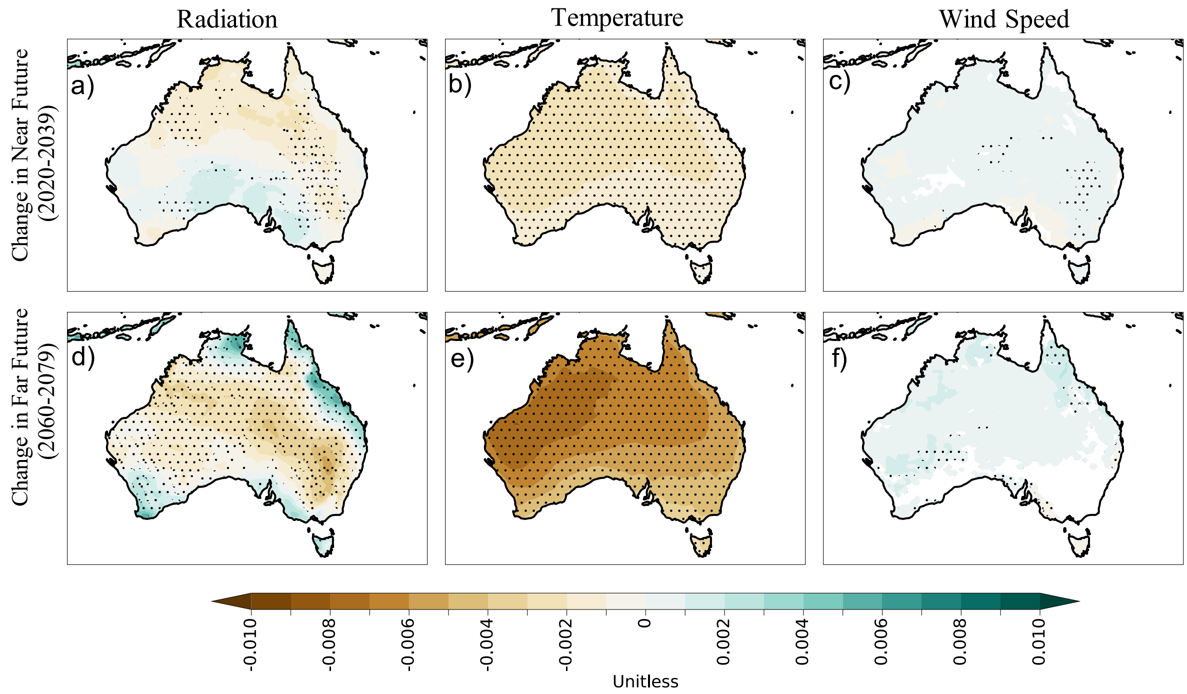

Figure s2*. Change in future PV potential due to shortwave downward radiation (a, d), daytime temperature (b, e) and daytime wind speed (c, f) over Australia for near future (a, b, c) and far future (d, e, f) period with respect to the historical period. Stippling indicates significant change (according to method 2.4).*

The individual contribution by the climatological variables (shortwave downward radiation, temperature and wind speed) towards the future change in PV potential shows that temperature influences the PV potential maximum in Australia followed by radiation and wind speed. Positive changes in the PV potential due to radiation majorly contribute towards the net small positive PV potential change over Australia.

6. Mean cell temperature over Australia for the historical period and relative changes in the cell temperature for the future periods

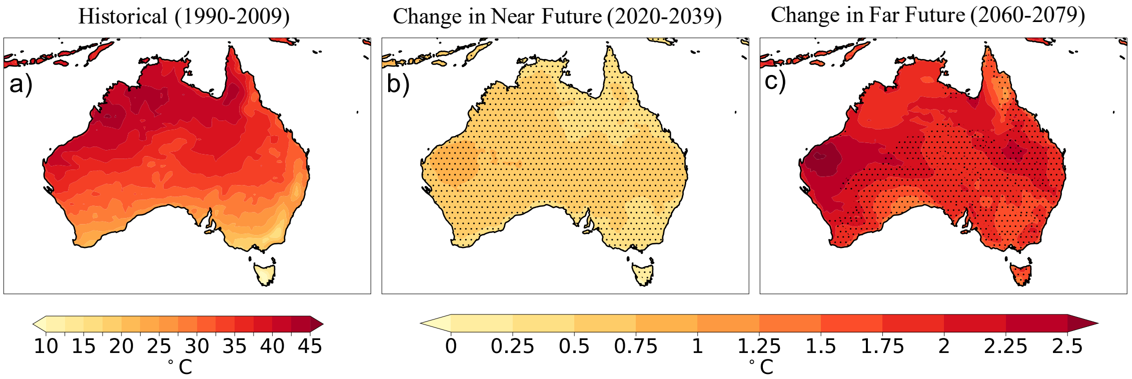

Figure s3 *a) Mean cell temperature over Australia for historical (1990-2009) period. Relative change in the mean cell temperature over Australia for b) near future (2020-2039) and c) far future (2060-2079) period with respect to the historical (1990-2009) period. Stippling indicates significant change (according to method 2.4).*

Australia records a mean cell temperature of around ~40-45 °C near the Northern Australia during the historical period. This mean cell temperature uniformly decreases (by ~5-10 °C) on moving towards the South of the continent. Due to climate change, an increase in around ~0.75-1 °C is expected during the near future period. Similar uniform rise in cell temperature (~1.5-2.5 °C) is expected for the far future period. The highest rise in the mean cell temperature is expected near the western part of the continent.

7. Cell efficiency loss

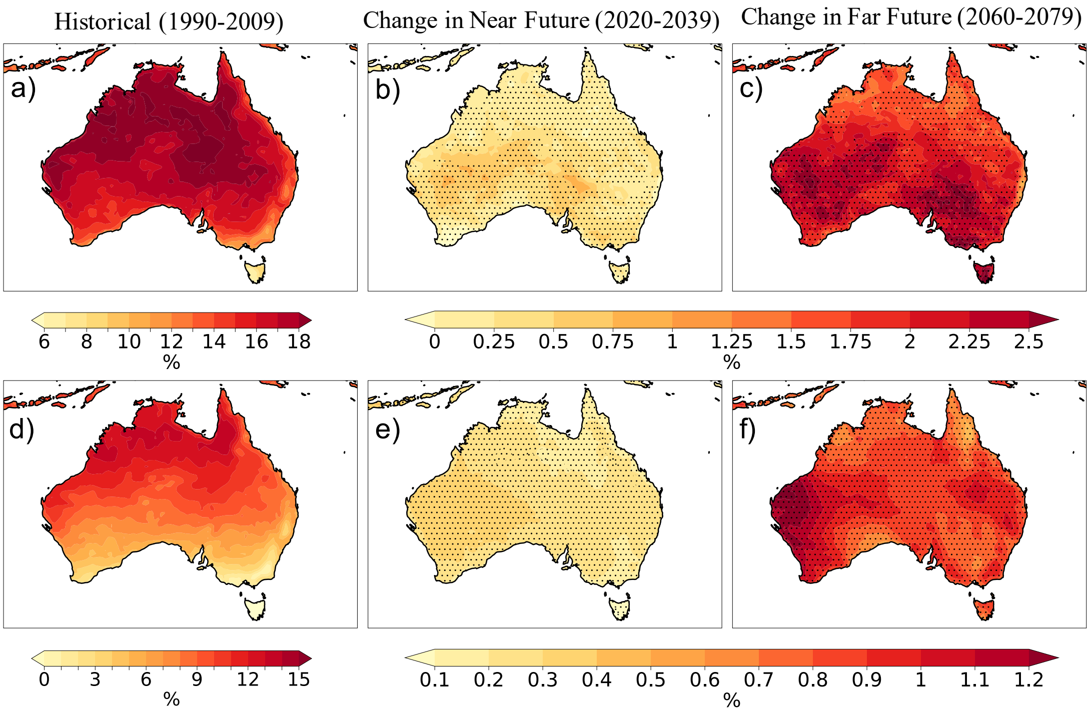

***Figure s4**. a) Annual maximum relative cell efficiency loss for historical (1990-2009) period. Change in the relative cell efficiency over Australia for b) near future (2020-2039) and c) far future (2060-2079) period with respect to the historical (1990-2009) period. d) Daily maximum relative cell efficiency loss for historical (1990-2009) period. Change in the daily maximum relative cell efficiency over Australia for b) near future (2020-2039) and c) far future (2060-2079) period with respect to the historical (1990-2009) period. Stippling indicates significant change (according to method 2.4).*

The annual maximum relative cell efficiency loss over Australia for the historical period is maximum over the Northern part of the continent with values going up to 17-18%. This loss increases during the near future period by ~1% and further increases by 2-2.5% during the far future period. Similar changes in the daily maximum relative cell efficiency loss are expected in the future periods. This loss increases during the near future and far future periods by 0.5% and 1.2% respectively.

8. Changes in the cell efficiency due to high cell temperature in future

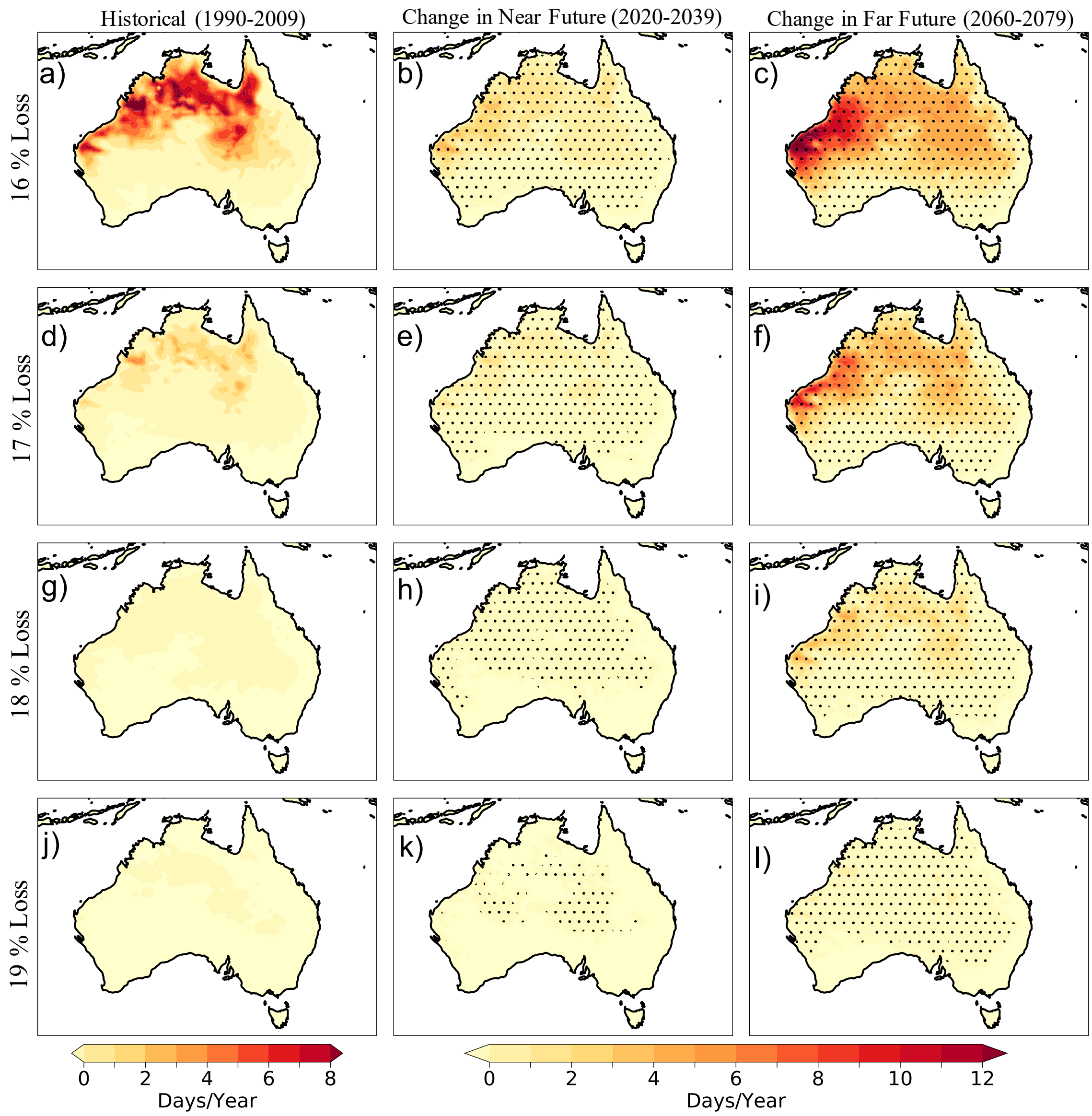

Figure s5. *Number of days/year cell temperature remains beyond threshold temperature for estimated loss in efficiency and there changes in the future periods.*

Reference

Chander, S., Purohit, A., Sharma, A., Arvind, Nehra, S. P., & Dhaka, M. S. (2015). A study on photovoltaic parameters of mono-crystalline silicon solar cell with cell temperature. *Energy Reports*, *1*, 104–109. https://doi.org/10.1016/j.egyr.2015.03.004

Evans, J. P., Ji, F., Lee, C., Smith, P., Argüeso, D., & Fita, L. (2014). Design of a regional climate modelling projection ensemble experiment - NARCliM. *Geoscientific Model Development*, *7*(2), 621–629. https://doi.org/10.5194/gmd-7-621-2014

Kaldellis, J. K., Kapsali, M., & Kavadias, K. A. (2014). Temperature and wind speed impact on the efficiency of PV installations. Experience obtained from outdoor measurements in Greece. *Renewable Energy*, *66*, 612–624. https://doi.org/10.1016/j.renene.2013.12.041

Makrides, G., Zinsser, B., Phinikarides, A., Schubert, M., & Georghiou, G. E. (2012). Temperature and thermal annealing effects on different photovoltaic technologies. *Renewable Energy*, *43*(June 2006), 407–417. https://doi.org/10.1016/j.renene.2011.11.046

Notton, G., Cristofari, C., Mattei, M., & Poggi, P. (2005). Modelling of a double-glass photovoltaic module using finite differences. *Applied Thermal Engineering*, *25*(17–18), 2854–2877. https://doi.org/10.1016/j.applthermaleng.2005.02.008